Correspondence

Imaging brine and air inclusions in sea ice using micro-X-ray computed tomography

Sea ice is a three-phase system consisting of ice, salt precipitates, liquid brine, and gas bubbles. Its heterogeneity affects both its physical properties (acoustic, electrical and optical) and its contributions to the biological and transport processes in the polar ecosystem and to global climate. Therefore the internal structure of sea ice has long been of interest to the scientific community. Primarily, optical methods have been used to examine porosity and brine networks in two dimensions (e.g. Light and others, 2003), although X-ray computed tomography was used as early as 1988 (Kawamura, 1988, 1990). Recently, however, advances in micro-X-ray computed tomography (micro-CT) have enabled the non-destructive examination of these features in three dimensions (3-D) on a much finer scale (Golden and others, 2007). This development has permitted advances in percolation theory using single crystals of sea ice doped with CsCl for X-ray contrast (Golden and others, 2007; Pringle and others, 2009).

We have recently developed a method to produce separate 3-D images of brine and air in natural polycrystalline sea ice using a SkyScan 1172 high-resolution micro-CT. The results make it possible to visualize and measure brine- and air-filled voids separately and together, and will lead to further discoveries of sea-ice properties.

MATERIALS AND METHODS

The sea-ice samples used for this illustration were collected from the Amundsen Sea in February 2008, where the in situ ice temperature was close to the freezing point. A sample 1.0 cm wide at the base and 2.5 cm tall was cut from the interior of a half-core section that had been shipped in dry ice and stored in the Dartmouth Ice Research Laboratory –10°C cold room that houses the SkyScan 1172 micro-CT. The sample was cut on a bandsaw, smoothed with a razor blade and mounted on a rotating stage in the micro-CT. The stage was rotated a full 360°, in 0.7° steps, with the micro-CT running at 40 kV, 250 μA and voxel size of 15 μm. Data processing included removal of ring artifacts and application of a symmetrical boxcar smoothing kernel. To reduce noise, we set smoothing to a value of 2, so that the grey values of every two pixels are averaged. Reconstruction of the X-ray attenuation data produced a stack of 971 1280 × 1280 voxel images (2.5 μm voxels in the vertical) in which the ice, brine and air could be easily distinguished (Fig. 1) due to their different X-ray attenuation characteristics and the range of intensities (4096) captured by the SkyScan 1172's 12-bit camera. In further analysis, these slices were binarized twice to highlight features of interest, with one threshold range for the voids, and a separate range for the brine pockets. To determine the grey-value range assigned to the different phases, we relied primarily on a visual comparison between the raw and binarized images. We have extensive experience examining firn in the SkyScan 1172, using the same scanning parameters and validating our thresholding by comparison of the reconstructed images to an image of the sample, sectioned and examined in a scanning electron microscope. Based on this, we set the range of grey values for pores to 0–70. We also knew, from examination of the sea-ice sample under an optical microscope, that the white areas in the reconstructed images were brine pockets or channels. Setting a threshold that included grey values of 174–255 produced the best match between these areas in the raw image and in the binarized image. The histogram of grey shades with these thresholds indicated is shown in Figure 2. Processing using these two separate thresholding ranges produced two separate sets of binarized images from which 3-D models could be built. The 3-D models were then colored differently so that, when recombined, the brine network and voids are easily distinguishable.

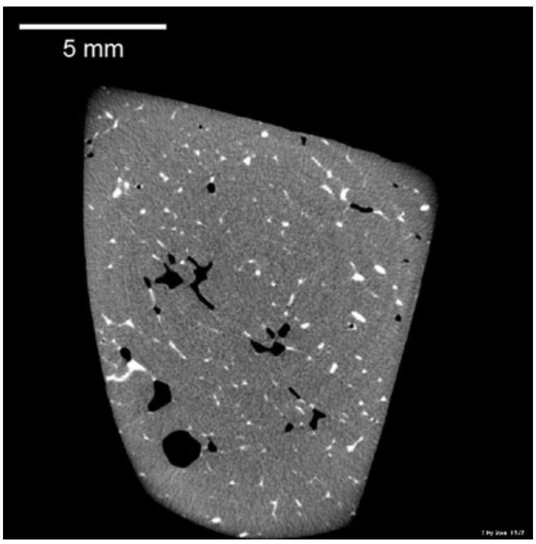

Fig. 1. Reconstructed greyscale image of a horizontal slice of the sample showing ice (grey), brine (white) and air (black). The sample is from 55 cm deep in an ice core from the Amundsen Sea.

RESULTS AND DISCUSSION

Figure 3 shows 3-D models of a volume of interest chosen from the center of the sample of Figure 1 from various viewing angles. The ice itself is black (not shown) so that the brine-filled areas (green) and air pockets (pink) can be clearly seen. Brine inclusions appear anisotropic and are elongated vertically, as previously observed (Weeks and Ackley, 1986;

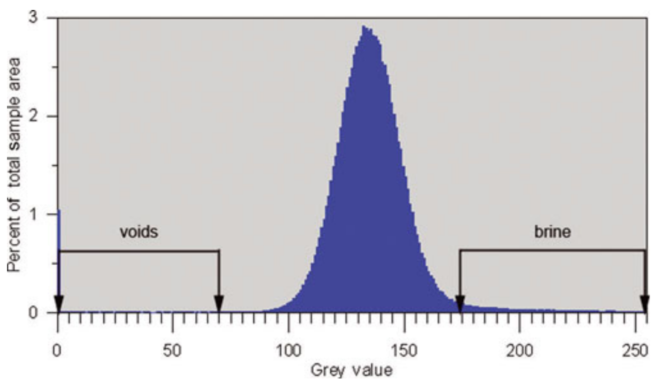

Fig. 2. Histogram of grey values of an 8 mm diameter circular area of interest from the image shown in Figure 1.

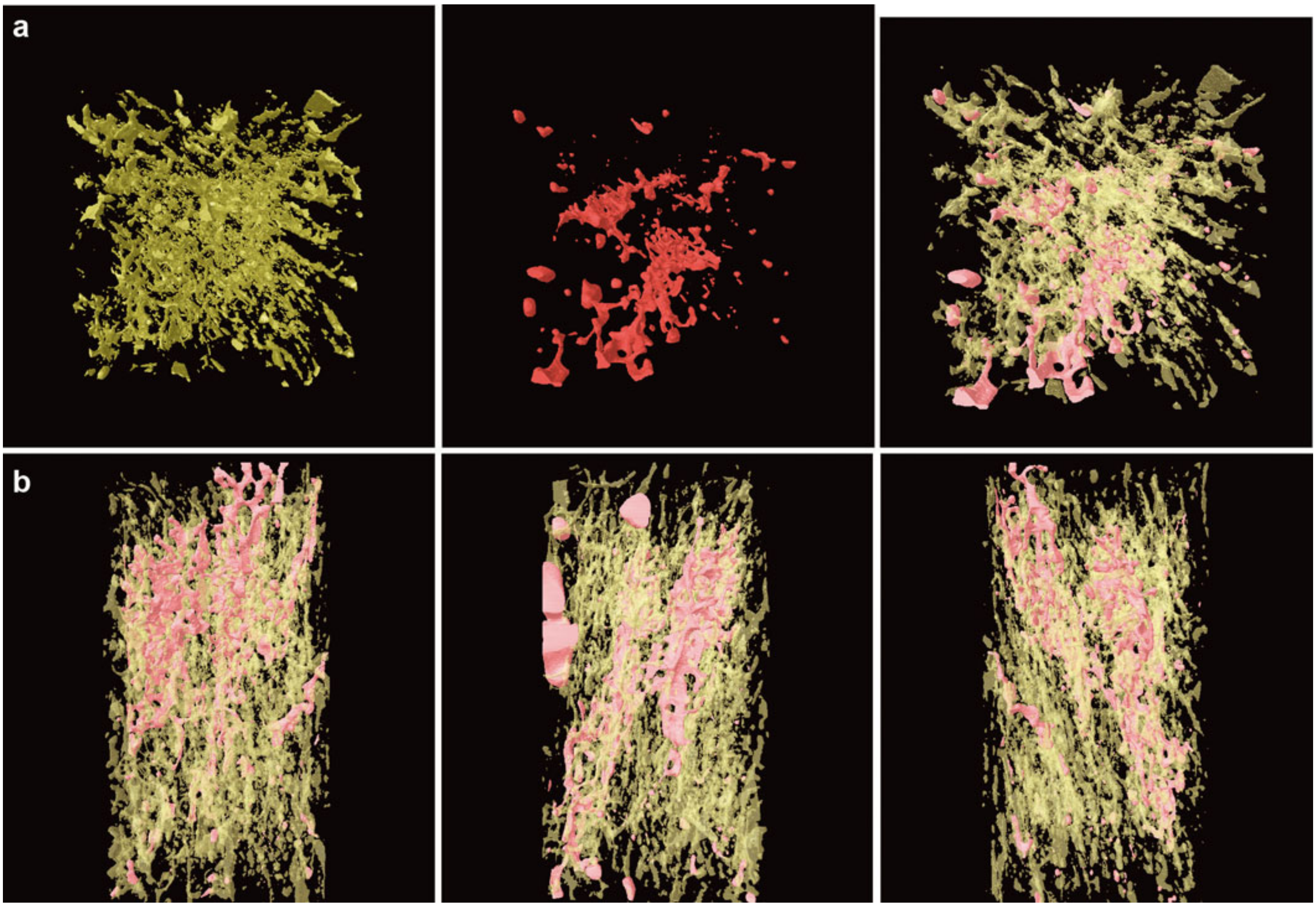

Fig. 3. Three-dimensional models of a 7.4 × 7.4 × 14.5 mm region of interest selected from the center of the sample. The ice itself is not shown, so that the interior brine (green) and air (red) can be seen. (a) Sample is shown from the top with first brine, then voids, then both together. (b) Vertical view of both brine and voids, shown from different angles.

Kawamura, 1988). Using the separate analyses of brine pockets and voids, we measured an air-pocket volume of 1.96% and a brine pocket volume of 2.50% of the total volume of interest. It should be kept in mind, however, that drained brine pockets will show up in X-ray attenuation images as voids. This ice was collected near the freezing temperature and initial drainage was significant. We took steps to prevent further drainage by transporting, storing and cutting the core at lower temperatures, and cutting a sample from the interior of the core. However, it is likely that drainage has affected the values given above. Future analysis of brine networks and void space, and calculations of porosity, brine and air-volume fraction and pore connectivity using micro-CT will require additional effort to prevent or account for drainage. Further, future work intended to produce reliable quantitative data will need to include a validation protocol for thresholding, such as comparison of the image stack with an optical or electron image of a cut surface of the sample (Kerckhofs and others, 2008). This would also prevent errors due to variations in grey values caused by using different imaging parameters on multiple samples.

CONCLUSION

Brine pockets and air-filled voids can be identified in natural sea ice using a micro-CT with a 12-bit charge-coupled device (CCD) detector. During post-processing, thresholds that take advantage of differences in the X-ray attenuation characteristics between ice and brine can be used to binarize images so that the two types of features are separated. Quantitative analysis resulting from this technique will be improved by calibration of the thresholding with a validation protocol. In future work, we plan to compare brine and void volume fraction obtained using micro-CT with chemical and physical properties measured on the sample using other means. This new technique will then be used to study spatial variations in sea-ice properties and transport processes as a function of time, temperature and chemistry.

ACKNOWLEDGEMENTS

Our micro-CT was acquired and this work supported by the US National Science Foundation grants OPP-0821056 and OPP-0738975 respectively. We thank E. Maksym of the British Antarctic Survey for supplying the sea-ice samples and E.M. Schulson for providing facilities in Dartmouth's Ice Research Laboratory.

Thayer School of Engineering, Rachel W. OBBARD
Dartmouth College, Gregory TRODERMAN
8000 Cummings Hall, Hanover, Ian BAKER
New Hampshire 03755, USA
E-mail: Rachel.w.obbard@dartmouth.edu

28 October 2009

REFERENCES

Golden, K.M., H. Eicken, A.L. Heaton, J. Miner, D.J. Pringle and J. Zhu. 2007. Thermal evolution of permeability and microstructure in sea ice. *Geophys. Res. Lett.,* **34**(16), L16501. (10.1029/2007GL030447.)

Kawamura, T. 1988. Observations of the internal structure of sea ice by X-ray-computed tomography. *J. Geophys. Res.,* **93**(C3), 2342–2350.

Kawamura, T. 1990. Nondestructive, three-dimensional density measurements of ice core samples by X ray computed tomography. *J. Geophys. Res.,* **95**(B8), 12,407–12,412.

Kerckhofs, G., J. Schrooten, T. van Cleynenbreugel, S.V. Lomov and M. Wevers. 2008. Validation of x-ray microfocus computed tomography as an imaging tool for porous structures. *Rev. Sci. Instr.,* **79**(1), 013711. (10.1063/1.2838584.)

Light, B., G.A. Maykut and T.C. Grenfell. 2003. Effects of temperature on the microstructure of first-year Arctic sea ice. *J. Geophys. Res.,* **108**(C2), 3051. (10.1029/2001JC000887.)

Pringle, D.J., J.E. Miner, H. Eicken and K.M. Golden. In press. Pore-space percolation in sea ice single crystals. *J. Geophys. Res.* (10.1029/2008JC005145.)

Weeks, W.F. and S.F. Ackley. 1986. The growth, structure, and properties of sea ice. *In* Untersteiner, N., *ed. Geophysics of sea ice*. New York, Plenum Press, 9–164.